university of groningen

University Medical Center Groningen

University of Groningen

Phase transformation of manganese-oxide precipitates in copper studied with transmission electron microscopy

Kooi, B.J.; de Hosson, J.T.M.

Published in:
Acta Materialia

DOI:
10.1016/S1359-6454(97)00419-9

IMPORTANT NOTE: You are advised to consult the publisher's version (publisher's PDF) if you wish to cite from it. Please check the document version below.

Document Version
Publisher's PDF, also known as Version of record

Publication date:
1998

Link to publication in University of Groningen/UMCG research database

Citation for published version (APA):
Kooi, B. J., & de Hosson, J. T. M. (1998). Phase transformation of manganese-oxide precipitates in copper studied with transmission electron microscopy. *Acta Materialia*, *46*(6), 1909 - 1922. https://doi.org/10.1016/S1359-6454(97)00419-9

Copyright
Other than for strictly personal use, it is not permitted to download or to forward/distribute the text or part of it without the consent of the author(s) and/or copyright holder(s), unless the work is under an open content license (like Creative Commons).

The publication may also be distributed here under the terms of Article 25fa of the Dutch Copyright Act, indicated by the “Taverne” license. More information can be found on the University of Groningen website: https://www.rug.nl/library/open-access/self-archiving-pure/taverne-amendment.

Take-down policy
If you believe that this document breaches copyright please contact us providing details, and we will remove access to the work immediately and investigate your claim.

Downloaded from the University of Groningen/UMCG research database (Pure): http://www.rug.nl/research/portal. For technical reasons the number of authors shown on this cover page is limited to 10 maximum.

Pergamon

Acta mater. Vol. 46, No. 6, pp. 1909–1922, 1998
© 1998 Acta Metallurgica Inc.
Published by Elsevier Science Ltd. All rights reserved
Printed in Great Britain
PII: S1359-6454(97)00419-9
1359-6454/98 $19.00 + 0.00

PHASE TRANSFORMATION OF MANGANESE-OXIDE PRECIPITATES IN COPPER STUDIED WITH TRANSMISSION ELECTRON MICROSCOPY

B. J. KOOI and J. TH. M. DE HOSSON

Department of Applied Physics, Materials Science Centre, University of Groningen, Nijenborgh 4, 9747 AG Groningen, The Netherlands

(Received 17 April 1997; accepted 27 October 1997)

Abstract—Manganese-oxide precipitates in Cu obtained by internal oxidation were studied using HRTEM. Internal oxidation of Cu–1 at.%Mn resulted in both MnO and Mn_3O_4 precipitates with as dominant facets parallel {111} of metal and oxide. In contrast to Ag where Mn_3O_4 nucleates directly, Mn_3O_4 in Cu is concluded to form out of MnO and the orientation relation between Mn_3O_4 and Cu is largely determined by the presence of an invariant line in the MnO and Mn_3O_4 lattices. Since Mn_3O_4 is thermodynamically more stable (also incorporating interfacial and strain energy) than MnO in Cu, the occurrence of MnO is ascribed to growth kinetics. © *1998 Acta Metallurgica Inc.*

1. INTRODUCTION

Metal–ceramic interfaces have a large and sometimes controlling influence on the properties of metal–ceramic composite materials. This influence then originates from a region a few atomic spacings wide and knowledge of the atomic structure in this region is therefore of great interest. HRTEM is particularly suited for the investigation of the atomic structure of interfaces and internal oxidation is a simple method to obtain clean interfaces between oxide precipitates and metal matrix. Then, the metal–oxide system under study and the conditions during oxidation determine the orientation relations (OR's) and the interface orientations (IO's) [1]. Internal oxidation of metals with several valence states (or which give polymorphic oxides) may result in the formation of oxide phases with various crystal structures and may involve phase transformations.

Within this framework, manganese oxide precipitates in Ag and Cu as obtained by internal oxidation were studied using HRTEM. A preceding paper reported about Mn_3O_4 precipitates in Ag [2] and particularly focused on the misfit-dislocation networks at parallel and tilted {111} Ag/Mn_3O_4 interfaces. MnO precipitates in Cu were already earlier investigated by HRTEM [1, 3]. Therefore, in this work attention is primarily focused on Mn_3O_4 precipitates in Cu. Principal difference between MnO and Mn_3O_4 precipitates within these f.c.c. metal matrices is that the former has a NaCl structure type and the latter has tetragonal structure (tetragonal distorted spinel, $I4_1/amd$). Hence, not only a misfit in size occurs between Mn_3O_4 and Ag or Cu lattices, as is the case for MnO and these metals, but also a misfit in shape. Moreover, a phase transformation from MnO to Mn_3O_4 which can be characterized (for the O lattice) by a Bain strain lattice correspondence occurs in Cu, whereas in Ag Mn_3O_4 appears to nucleate directly. The present paper primarily addresses the oxide-phase development and orientation relations between precipitates and metal matrix upon internal oxidation of a Cu–1 at.%Mn alloy in close comparison with the internal oxidation in the Ag matrix. In another paper the misfit-dislocation structure at interfaces between Cu and MnO or Mn_3O_4 is considered [4].

2. EXPERIMENTAL

An alloy of copper containing 1 at.% manganese was made in a high-frequency furnace by melting the pure constituents (purity 99.99 wt%) in an alumina crucible under oxygen-free argon protective atmosphere. The ingot was homogenized (1 week 700°C) and subsequently cold rolled from 4 mm down to 0.5 mm. Oxidation was performed in a Rhines pack [5, 6] (Cu-foil containing Cu, Cu_2O and Al_2O_3 powder in volume ratio of about 1:1:1) at 1000°C (2 h), 900°C (5 and 20 h) and 800 C (24 h) in an evacuated quartz tube. The oxidation times, except 20 h at 900°C, were chosen such to allow in all cases a comparable oxidation penetration depth (order of the thickness of the specimen). Oxidation of Cu–1 at.%Mn (5 h 900°C) was also carried out in Rhines packs consisting of Cu/CuO (volume fraction about 1:2) and Cu/Cu_2O (vol. fr. 2:1).

TEM samples were prepared by grinding, dimpling and ion milling 3 mm discs to electron trans-

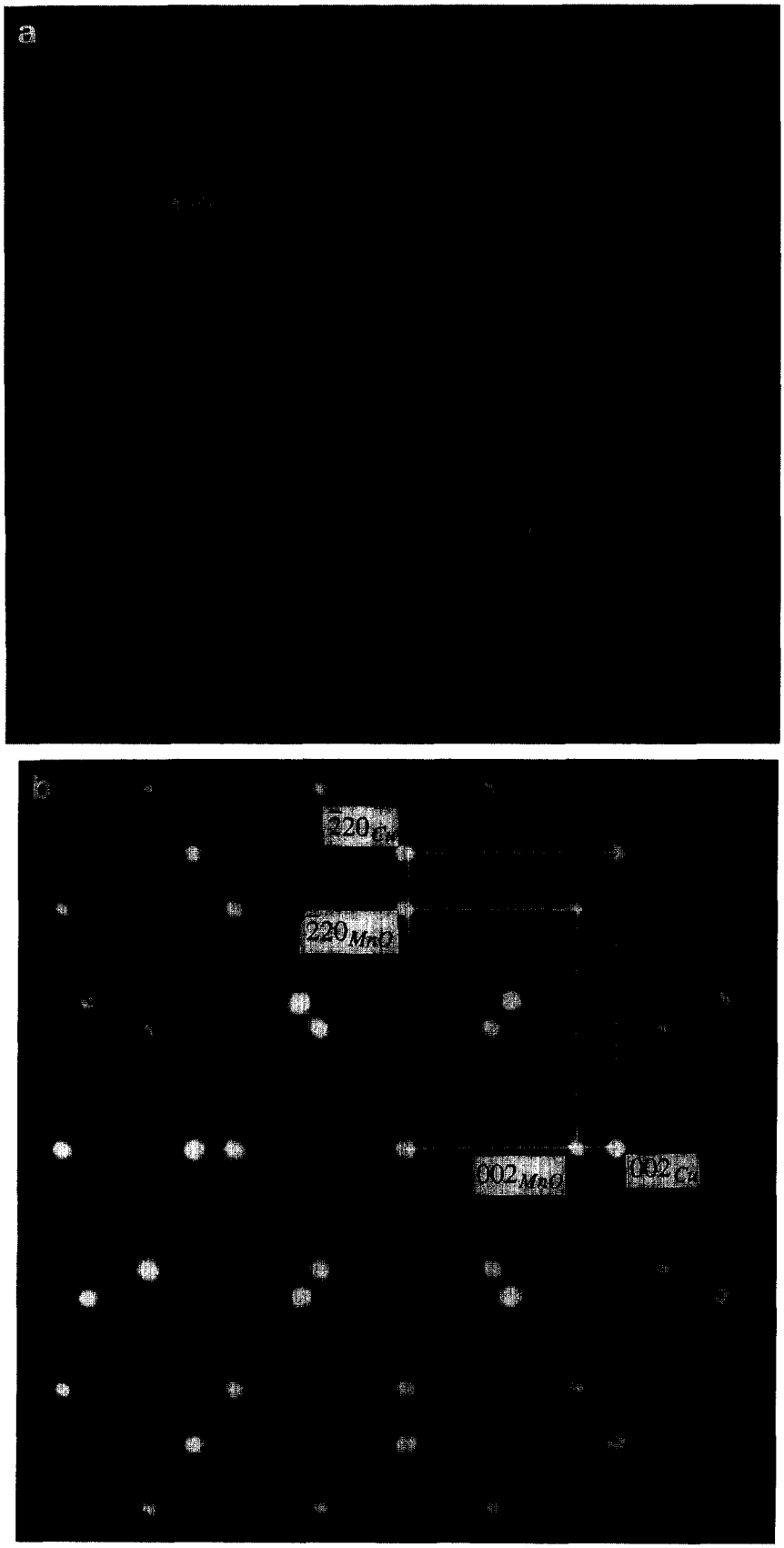

Fig. 1(a–b). *Caption opposite.*

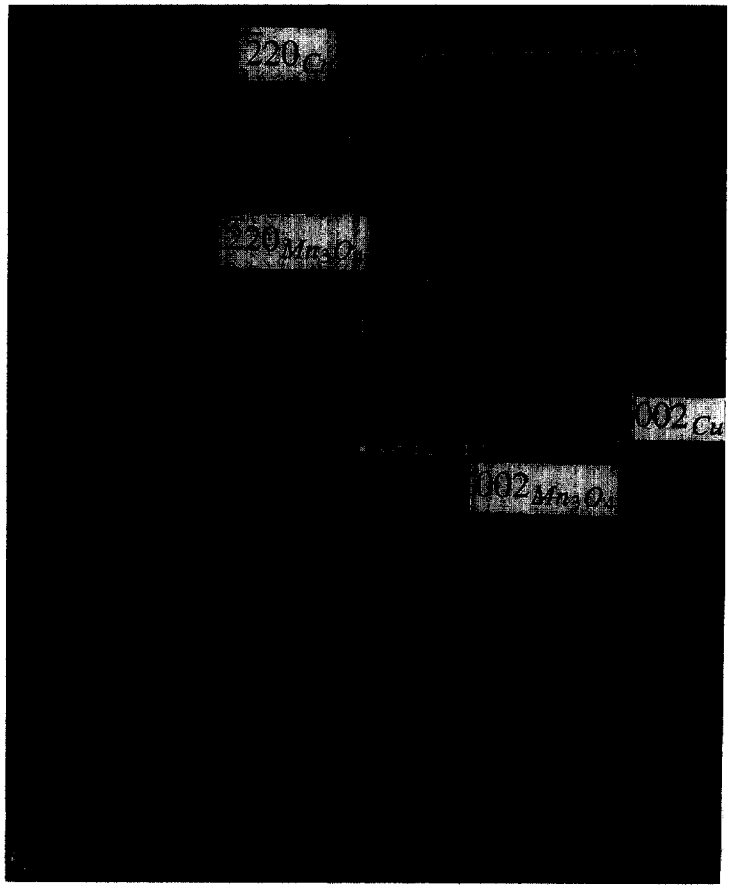

Fig. 1. (a) Bright-field image showing a MnO (bright) and a Mn_3O_4 (dark) precipitate with octahedron shape due to 8 {111} facets in Cu as viewed along the [110] of Mn_3O_4. (b) ⟨110⟩ zone axis SAED pattern of MnO in Cu showing parallel topotaxy. (c) The SAED pattern of the Mn_3O_4 precipitate in Cu corresponding to (a) showing a parallel topotaxy; due to the tetragonality of Mn_3O_4 the [110] of Mn_3O_4 (viewing direction) and Cu are misaligned by 4.1° leading to parallelism of $(111)[01\bar{1}]$ for Cu and Mn_3O_4.

parency. For HRTEM a JEOL 4000 EX/II, operating at 400 kV (spherical aberration coefficient: 0.97 ± 0.02 mm, defocus spread: 7.8 ± 1.4 nm, beam semi-convergence angle: 0.8 mrad) was used.

3. RESULTS

Internal oxidation of Cu–1 at.%Mn in a Rhines pack (Cu_2O, Cu and Al_2O_3 powder) at 1000°C (2 h), 900°C (5 h) and 800°C (24 h) resulted for all three temperatures in MnO (NaCl structure type) and a minor amount of Mn_3O_4 (tetragonal distorted spinel, I4/amd [7]) precipitates (see Figs 1–3). In most cases a precipitate consisted completely of one phase (*cf.* Figs 1–3), but also some precipitates comprised both MnO and Mn_3O_4. An example of this latter case is shown in Fig. 4. The interface between MnO and Mn_3O_4 does not seem to be sharply facetted. However, this does not have to be actually the case, because the facet can be inclined to the viewing direction. Variations in foil thickness then give rise to a blurred contrast.

In contrast to MnO precipitates, which were each always single-crystalline, a significant fraction ($30 \pm 10\%$) of Mn_3O_4 precipitates consisted of several domains. Often these domains were variants related by tetragonal twinning, *i.e.* with twin boundaries parallel to {011}. Note that in the present paper for purpose of maximum similarity with MnO and the f.c.c. metals, Laue indices of Mn_3O_4 are based on tetragonal spinel and not on I4/amd which has a smaller unit cell; *i.e.* [100] and [010] for tetragonal spinel corresponding to [110] and $[\bar{1}10]$ for I4/amd. An example of such a tetragonally twinned Mn_3O_4 precipitate with the twin boundaries observed edge-on as viewed along the [111] zone axis of Mn_3O_4 is given in Fig. 5. Also, Mn_3O_4 parts of partially transformed MnO precipitates can already exhibit tetragonal twinning as is shown in Fig. 6. For more details about tetragonal twinning in Mn_3O_4 precipitates in both Ag and Cu matrices, see Ref. [8]. Besides tetragonal twin boundaries, other less regular grain boundaries, which have not been studied in detail, but could be characterized as low-angle grain boundaries were often observed in

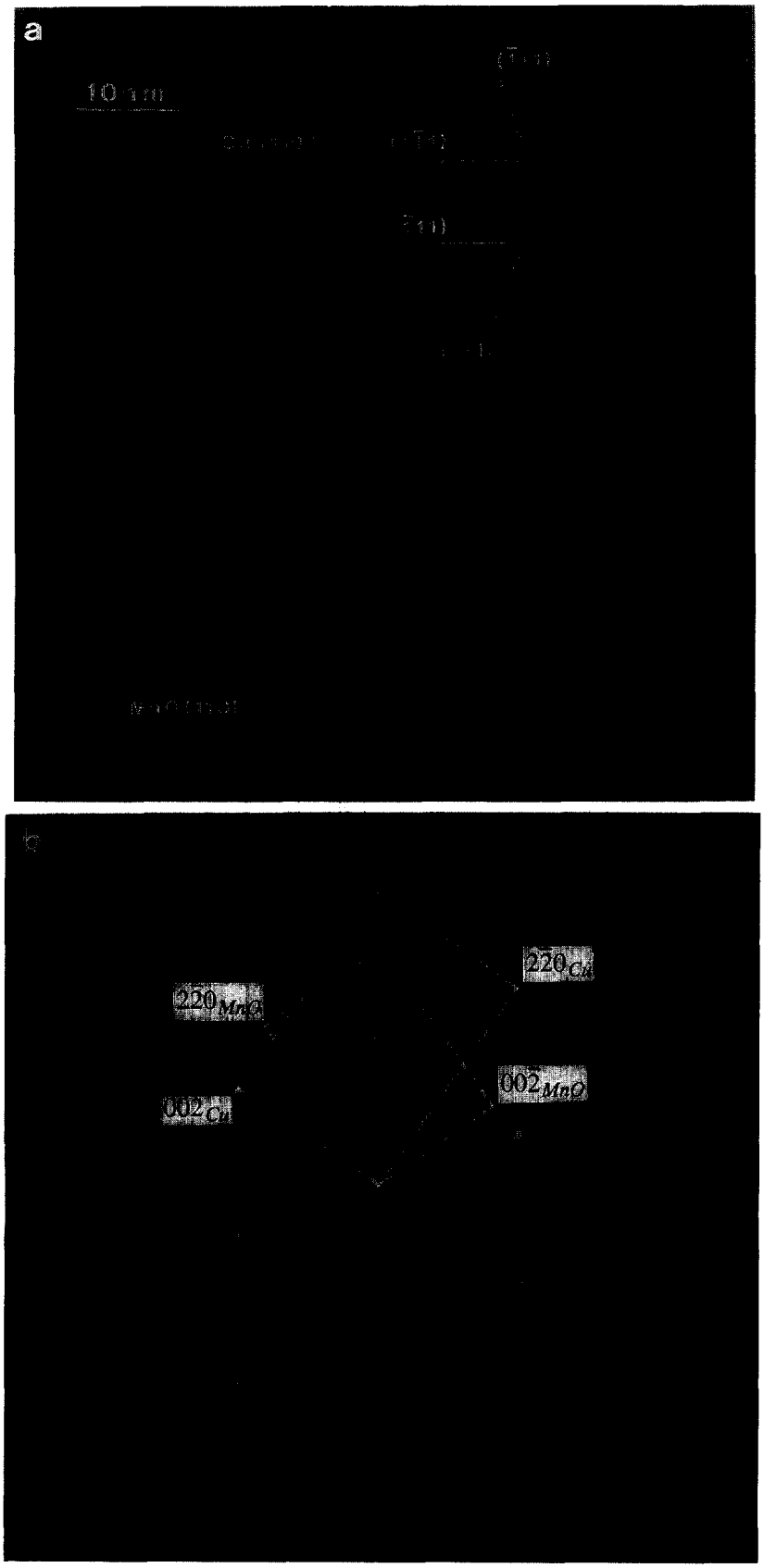

Fig. 2. (a) HRTEM image, with view along [110], showing a part of an MnO precipitate in Cu with plate shape due to one pair of dominant (111) facets. (b) The corresponding SAED pattern showing twin topotaxy (71 ⟨110⟩).

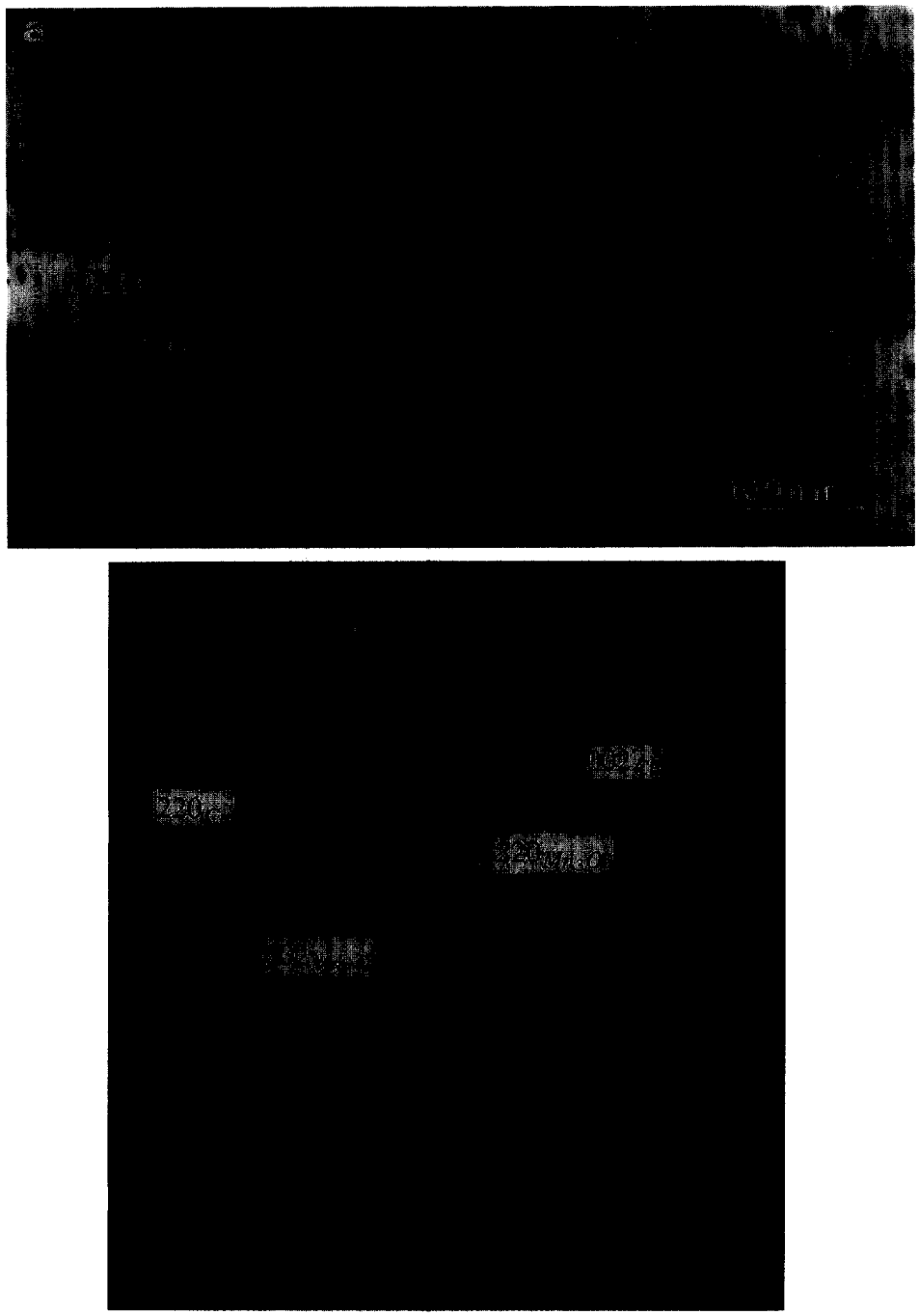

Fig. 3. (a) Bright-field image of an Mn_3O_4 precipitate in Cu with plate shape due to one pair of dominant $(1\bar{1}1)$ facets, viewed along the [110] of Mn_3O_4. (b) The corresponding SAED pattern showing twin topotaxy (71°⟨110⟩); due to the tetragonality of Mn_3O_4 both the [110] of Mn_3O_4 (viewing direction) and Cu and the $(1\bar{1}1)$ of Cu and Mn_3O_4 (the dominant facet of the precipitate) are not aligned parallel.

the Mn_3O_4 precipitates. An example of such a 'polycrystalline' Mn_3O_4 precipitate is given in Fig. 7. It shows a bright-field image of an Mn_3O_4 precipitate in Cu viewed along [100]. The precipitate consists of 2 major domains, with only one domain exactly in the [100] zone axis and both domains are tetragonally twinned. The Cu[100] is 2.8° off-axis. The two domains appear to be a result of two different nucleation sites for Mn_3O_4 in the original MnO precipitate and with different OR's between Mn_3O_4 and the original MnO for the two domains. Below, it will be discussed in more detail that, starting from one OR between MnO and Cu, the corresponding transformed Mn_3O_4 in Cu can arise with different variants of this OR which are related by rotations of the order of a few degrees.

The precipitates have a typical size of 200 nm for all oxidation temperatures; for comparison the Mn_3O_4 precipitates in Ag have a size 5–25 nm [2]. This difference between Cu and Ag in precipitate size is mainly due to a larger difference in affinity for oxygen between Ag and Mn than between Cu and Mn. The Mn_3O_4 precipitates in Cu appeared to be significantly larger on average than the MnO precipitates.

Oxidation of Cu–1%Mn (5 h, 900°C) in Rhines packs consisting of Cu/CuO (volume fraction about 1:2) and Cu/Cu_2O (vol. fr. 2:1) resulted in the formation of only MnO and of both MnO and Mn_3O_4, respectively.

The OR between the precipitates and the Cu matrix found predominantly for the different oxidation temperatures is parallel topotaxy, *i.e.* cube-on-cube for MnO in Cu and for Mn_3O_4 in Cu only few planes and directions can be parallel simultaneously, analogous to Mn_3O_4 in Ag [2] (see Fig. 1). Then, the precipitates have octahedron shapes due to {111} facets and in case of MnO also very small {100} facets, *i.e.* a truncated octahedron. This OR and facetting was earlier observed for *e.g.* MgO precipitates in Cu [9–12] and Pd [9, 11] and CdO in Ag [13]. The ratio of {100} to {111} facet area is significantly larger for MgO than for MnO in Cu. The ratio of the interfacial energies of {100} and {111} thus increases for MgO, MnO and Mn_3O_4 in Cu and is larger than $\sqrt{3}$ for the last due to the absence of truncation and about 1.3 for MgO [14]. In Cu–Mn oxidized at 800°C also a significant fraction of precipitates have 71°⟨011⟩ OR, *i.e.* twin topotaxy (see Figs 2–4). At 900 and 1000°C this OR is also, but rarely, observed in Cu. For this OR the precipitate is plate-shaped with parallel {111} of metal and oxide as dominant facet. Other OR's observed with a low frequency in Cu are: $(1\bar{1}1)_{metal}\|(3\bar{1}0)_{oxide} + [110]_{metal}\|[130]_{oxide}$, 55°⟨011⟩ and 90°⟨011⟩. An important factor determining that only a single OR is possible in Ag (*cf.* Ref. [2]), whereas more OR's are observed in Cu is probably the precipitate size (which is a direct consequence of the difference in oxygen affinity of manganese and the metal matrix). The smaller the precipitate size the more the surface and strain energy pose restrictions on allowable interface orientations and hence orientation relations.

Since Mn_3O_4 is tetragonal the above OR's are only accurately specified for Mn_3O_4 and Cu, if the direction(s) and plane(s) which are actual parallel for the two phases are specified. For instance, the parallel topotaxy for MnO/Cu is observed and interpreted to be present in slightly different variants for Mn_3O_4/Cu with actual parallelism of:

(i) the principal axes ({hk0}⟨001⟩ + {001}⟨hk0⟩)
(ii) {011}⟨100⟩
(iii) {111}⟨01$\bar{1}$⟩
(iv) {133}⟨01$\bar{1}$⟩.

The variants (i) to (iv) seem to correspond to quite different OR's, but in practice they are only related by small rotations. Starting from (i), (ii) is

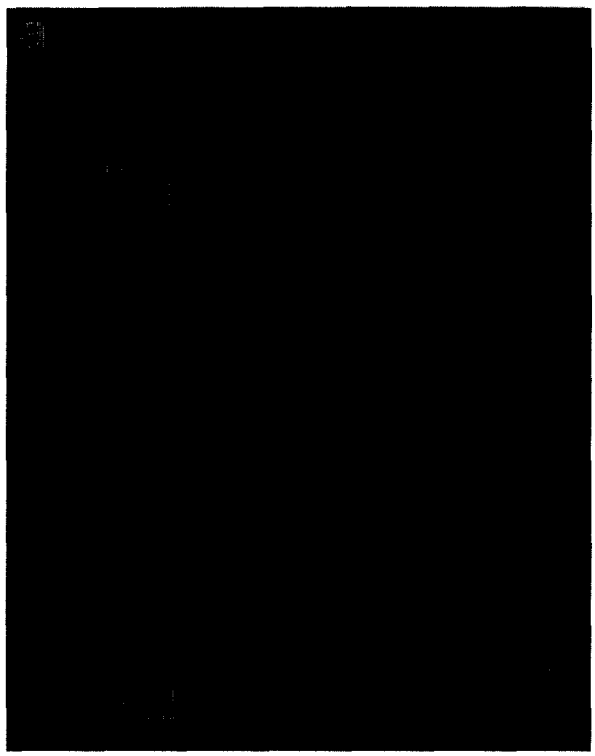

Fig. 4a. *Caption opposite.*

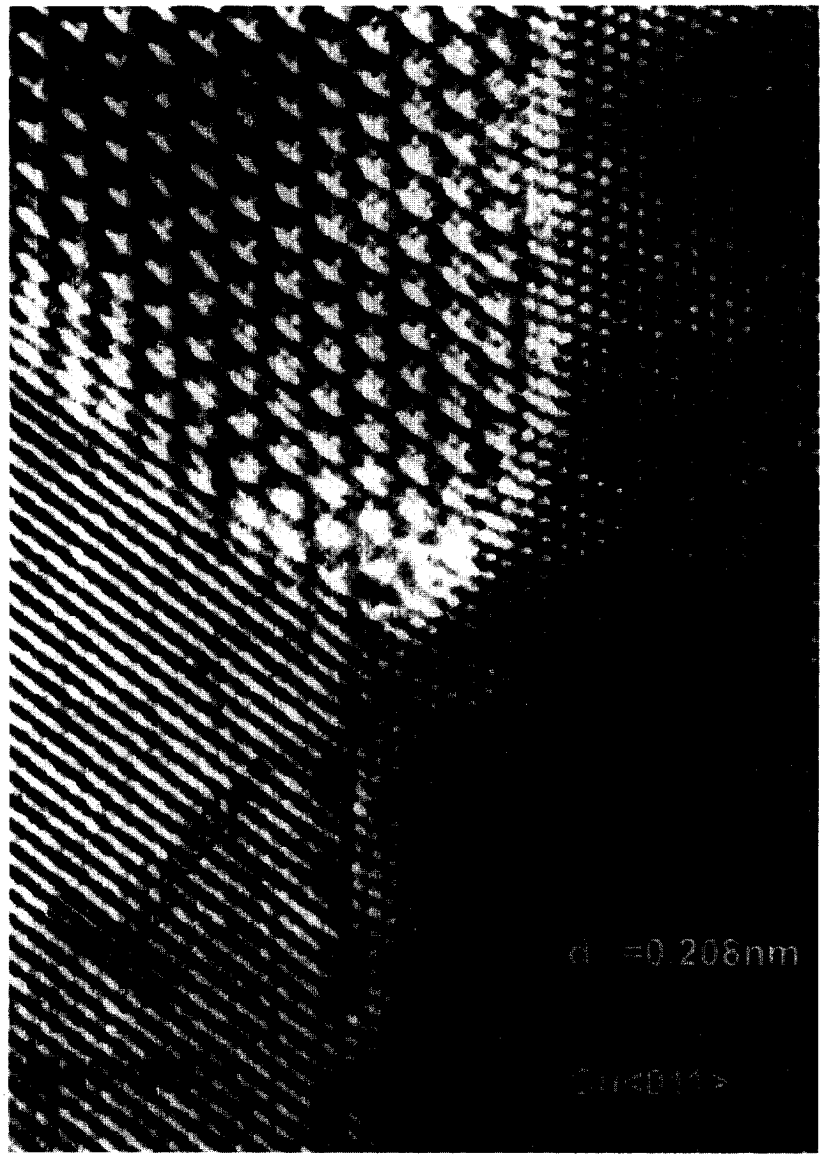

Fig. 4. (a) HRTEM image, with view along [011], showing an MnO precipitate in Cu with twin topotaxy which for a part has been transformed into Mn_3O_4. (b) Detail of image shown in (a).

obtained by a rotation of 4.16° around ⟨100⟩, then (iii) and (iv) are obtained from (ii) by rotations around $\langle 01\bar{1}\rangle$ of 1.85° and 0.89°, respectively. These values for the rotation suggest an accuracy which was not achieved experimentally. Rotations could be observed experimentally by aligning zone axes of Mn_3O_4 and the surrounding Cu using Kikuchi patterns parallel to the electron beam, recording SAED patterns and determining with the goniometer stage the angle difference and direction of rotation, as often was the case, between the zone axis of Mn_3O_4 and the corresponding one of the surrounding Cu. In the most favorable case, *i.e.* least difficulty with interpretation, the zone axes of Mn_3O_4 and Cu were observed parallel. Then the accuracy concerns the rotation around this parallel axis as observed in SAED patterns, which is in favorable cases about 0.5°. OR (ii) was predominantly observed for precipitates showing tetragonal twinning and then the twinning plane corresponded to the parallel {011}. OR (iii) was more frequently observed for the plate-shaped precipitates (near to 71°⟨011⟩ OR) than for precipitates with octahedron shape (near to parallelism of principal axes) and then in general the dominant {111} facet of the plate corresponded to the parallel {111}.

4. DISCUSSION

4.1. Precipitate formation in Cu and a comparison with Ag

In Cu on passage of the oxidation front first MnO nucleates which in a later stage transforms

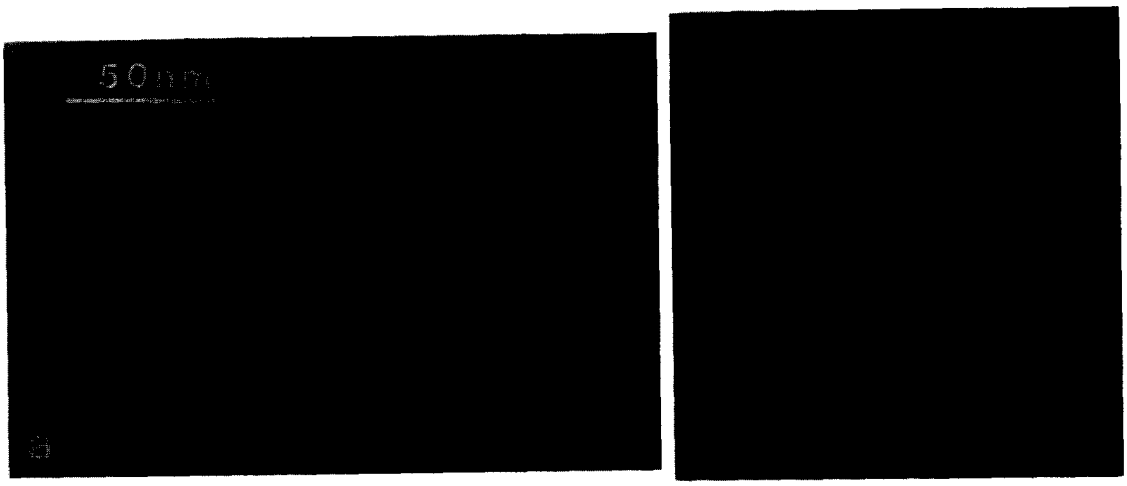

Fig. 5. Tetragonally twinned Mn_3O_4 precipitate in Cu viewed along the [111] with 7 twin planes edge on. (a) Bright-field image. (b) Selected-area electron diffraction pattern.

into Mn_3O_4, but yielding a large intermediate region in which both MnO and Mn_3O_4 are present, as can be seen in Fig. 1, where precipitates of both phases exist next to each other. The successive formation of an oxide with lower and higher oxidation state with an intermediate region containing both oxide phases was observed earlier for, *e.g.*, internally oxidized Co–Ti [15] and Ag–Cu [16]. The coexistence of MnO and Mn_3O_4 in a precipitate; observed in several cases; indicates this ongoing transformation (*cf.* Figs 4 and 6). A reverse transformation of Mn_3O_4 into MnO is only expected in a reducing atmosphere (which was indeed achieved for directly nucleated Mn_3O_4 precipitates in Ag which could be reduced to MnO) and is inconceivable in an oxidizing atmosphere. The generally larger size of Mn_3O_4 compared to MnO precipitates in Cu probably reflects the volumetric expansion per Mn atom that occurs during the MnO to Mn_3O_4 transformation.

Evidence for the transformation can be found in the many polycrystalline Mn_3O_4 precipitates (not

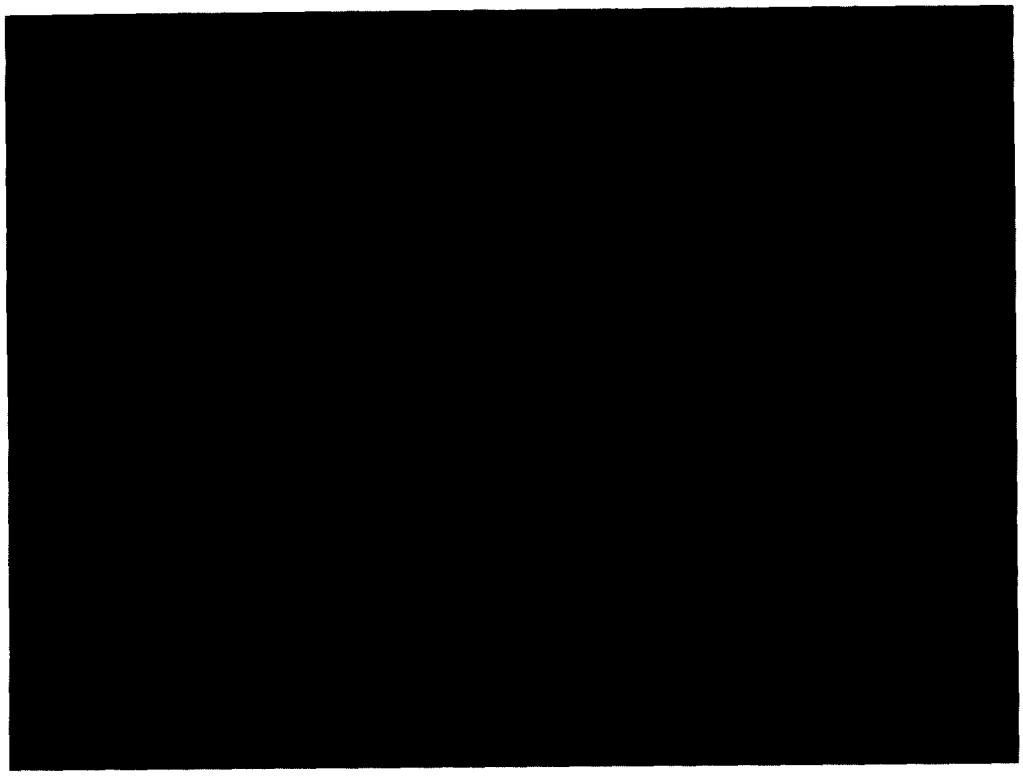

Fig. 6. HRTEM image, with view along [111], showing a detail of an MnO precipitate in Cu with parallel topotaxy which for a part has been transformed into tetragonally-twinned Mn_3O_4.

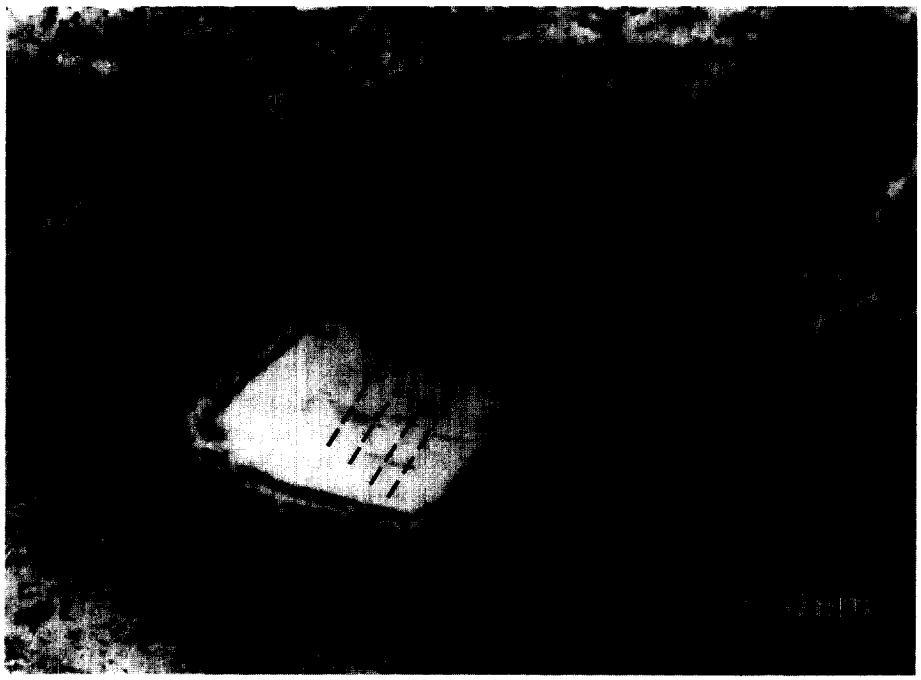

Fig. 7. Bright-field image of an Mn_3O_4 precipitate in Cu viewed along [100]. The precipitate consists of 2 major domains, with only one domain exactly in the [100] zone axis and both domains are tetragonally twinned. Two edge on observed twin planes are indicated by solid lines and traces of some inclined twin boundaries are indicated by dashed lines. The Cu[100] is 2.8° off-axis.

including tetragonal twinned precipitates as polycrystalline) with low-angle grain boundaries found in Cu. In contrast, the MnO precipitates in Cu and the Mn_3O_4 precipitates in Ag, which in both cases are interpreted to have been nucleated directly, were always single-crystalline. The shape of these polycrystalline Mn_3O_4 precipitates in Cu is such that they are not the result of separately nucleated Mn_3O_4 parts which have grown together. The only possible way in which these precipitates could have formed is that first a single-crystalline precipitate was formed with well-defined shape (generally an octahedron) which in a second step broke up in differently oriented parts. This breaking up can only be understood if the original single-crystalline precipitate was MnO which subsequently transformed in Mn_3O_4 with more than one nucleation site for the Mn_3O_4. The tetragonality of Mn_3O_4 with respect to the cubic parent phase makes it possible that a single orientation relation (OR) between MnO and Cu changes into different variants between Mn_3O_4 and Cu. These different variants were indeed observed (see Section 3). In some cases it may be possible that such a polycrystalline Mn_3O_4 precipitate reduces its internal interfacial energy by a further growth of one of the crystallites at the expense of the others. Then a single-crystalline Mn_3O_4 precipitate can result. However, the Cu matrix may prevent this growth if the Cu/Mn_3O_4 interfacial/strain energy increases and dominates over the internal interfacial energy in the Mn_3O_4. Instead of more than one nucleation sites for Mn_3O_4 per MnO precipitate often only one nucleation site which subsequently 'consumed' the whole MnO precipitate will have occurred. Then single-crystalline Mn_3O_4 precipitates were formed.

With the above it can not be excluded that direct nucleation of Mn_3O_4 occurred, *i.e.* without MnO as an intermediate. However, retardation of the oxidation process (see below) gave rise to solely MnO and therefore it is likely that all Mn_3O_4 originate from transformation out of MnO, but when observed in a relatively later stage of the process this transformation has already started.

In Ag Mn_3O_4 appeared to nucleate directly. A reason for the absence of MnO in Ag, compared with its presence in Cu, may be a difference in partial pressure of oxygen during oxidation of Ag and Cu. The higher oxygen pressure for internal oxidation in the Ag matrix may favor direct Mn_3O_4 nucleation. To verify this Ag–3 at.%Mn was oxidized, with a Rhines pack (Cu_2O, Cu and Al_2O_3 powder in Cu foil) separately present, in an evacuated quartz tube. However, instead of internal oxidation, external oxidation occurred giving rise to a predominantly MnO scale. Since Mn_3O_4 is also ultimately formed in Cu the oxygen pressure is sufficiently high to form this phase for both Ag and Cu. Instead of a difference in oxygen pressure, the difference between Ag and Cu in the oxygen (relative to the manganese) permeability (*i.e.* $c_O D_O$ and $c_{Mn} D_{Mn}$ with c_O and c_{Mn} the oxygen and manganese concentration in the metal matrix and D_O and D_{Mn} their respective diffusion coefficients in this

matrix) is a more probable explanation for the Mn_3O_4 nucleation in Ag and the MnO nucleation in Cu. At 900°C, $c_O D_O$ is about two orders of magnitude larger in Ag than in Cu [17]. The much more rapid supply of oxygen in Ag than in Cu to each Mn atom (and difficult dissociation of oxide molecules formed; more difficult in Ag than in Cu due the larger difference in oxygen affinity with Mn) can very well explain the direct nucleation of Mn_3O_4 in Ag, whereas first MnO nucleates in Cu.

Oxidation of Cu–1 at.%Mn (5 h 900°C) in Rhines packs consisting of Cu/CuO (volume fraction about 1 : 2) and Cu/Cu_2O (vol. fr. 2 : 1) resulted in the formation of only MnO and of both MnO and Mn_3O_4, respectively. This seems contrary to the expectation that a higher partial pressure of oxygen results in an oxide with higher oxidation state. However, internal oxidation of Cu-based alloys in CuO containing Rhines Packs will lead to a more severe oxidation of at least the exterior of the Cu sample. This oxide probably retards the transport of oxygen to the interior of the sample and then retards the internal oxidation process. This view is supported by the observations that the oxygen permeability in Cu matrix alloys is about 20% higher for oxidation in a Rhines pack than in case also external oxidation occurs in air [18].

These considerations on MnO and Mn_3O_4 formation in Ag and Cu have kinetic background. From a thermodynamic point of view the change in Gibbs-free energy consisting of superposition of bulk, interfacial and strain energy terms determines which oxide phase is most favorable to form. The change in Gibbs-free energy (without accounting for interfacial and strain energy) for the formation of MnO, Mn_3O_4, β-Mn_2O_3 (Ia3) and MnO_2 (P4/mnm) out of Mn and O_2 is shown in Fig. 8 as a function of temperature per unit of volume (a) and per mole Mn (b) (data from Ref. [19]). From Fig. 8(a) it is evident that, if the matrix allows growth of a precipitate within a certain volume or if the Gibbs-free energy is defined per oxygen atom (*e.g.*, if the supply of oxygen is rate determining). MnO formation is preferred. However, per Mn atom oxidation to higher oxidation states is more favorable and since after sufficient long oxidation times only the Mn concentration is limited this will eventually be the case (b).

For the internal oxidation temperatures 800 and 900°C, β-Mn_2O_3 has lowest bulk energy. The mismatch between the lattice constants of Ag or Cu and β-Mn_2O_3 is significantly larger than between Ag or Cu and either MnO or Mn_3O_4. This makes β-Mn_2O_3 less favorable for coherent and semi-coherent precipitates in these metals. Further, unlike MnO and Mn_3O_4, β-Mn_2O_3 does not form a completely filled close-packed layer of oxygen ions at the metal–oxide interface. It will be shown below that this is of substantial importance and makes β-Mn_2O_3 again less likely to occur.

From the viewpoint of strain energy on most interfacial faces, Mn_3O_4 in these metals gives rise to the lowest energy. This is demonstrated by anisotropic linear elasticity calculations (elastic constants from Ref. [20]) on interfaces between MnO or Mn_3O_4 and Cu; the results of which are presented in Table 1 together with results from atomistic calculations on interfacial energies (differences are mainly due to strain energy; these calculations are discussed in Ref. [4]). Since the difference in interfacial energy between MnO and Mn_3O_4 in each of these metals is probably small, both oxides are terminated by a close-packed oxygen layer and thus only a difference in second nearest neighbor interaction across the interface occurs, and since both bulk and strain energy is lower for Mn_3O_4, this phase is expected.

The initial formation of MnO in Cu is thus, based on the above thermodynamic and kinetic arguments, determined by growth kinetics.

The presence of MnO and Mn_3O_4 precipitates next to each other is not at variance with Mn_3O_4 transforming out of MnO. In other systems where during internal oxidation the oxide precipitates

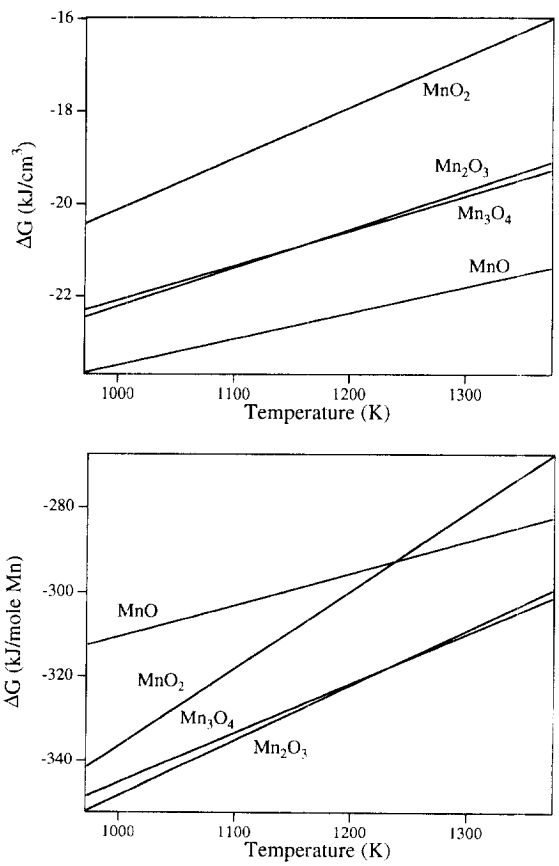

Fig. 8. Change of the Gibbs-free energy for the bulk oxidation of Mn into several oxide phases as indicated [MnO, Mn_3O_4, β-Mn_2O_3 (Ia3), MnO_2 (P4/mnm)] (a) Gibbs-free energy change per unit volume oxide formed. (b) Gibbs-free energy change per mole Mn reacted.

Table 1. Strain energy on Cu/MnO and Cu/Mn_3O_4 interfaces for parallel interface orientation and different interfacial planes as calculated with anisotropic linear elasticity

Cu‖		MnO	Mn_3O_4
Elasticity		(GPa)	(GPa)
	{100}	1520	1370
	(001)	1520	460
	{111}	1701	1171
Atomistics		(mJ/m^2)	(mJ/m^2)
	{111}	−888 (25% mismatch), −1041 (20% mismatch)	−1099 (mismatch: 12.5% in [110], 25% in [11$\bar{2}$])

Interfacial energy for parallel {111} Cu/MnO and Cu/Mn_3O_4 interfaces according to the atomistic calculations. At the Cu/MnO interface an isotropic strain of 25 or 20% was assumed (is actually 22.9%) and at the Cu/Mn_3O_4 interface a strain of 12.5% was taken in the [110] and 25% in the [11$\bar{2}$]. The factor α allowing simulation of different interaction strengths across the interface (see Ref. [4]) was given a value 2.

exhibited a phase transformation (see Refs [15, 16] in the paper) relative large regions were observed in which both phases can exist next to each other. Apparently the rate of transformation can be very different for different precipitates; it is a statistical process where only a fraction of precipitates have overcome the activation-energy barrier for transformation. The difference in stability between MnO and Mn_3O_4 with respect to Cu_2O is relatively small and therefore the rate of transformation is expected to be very slow, *i.e.* the fraction of transformed precipitates increases only very slowly. Both MnO precipitates and fully transformed Mn_3O_4 precipitates are more stable than partially transformed precipitates. Therefore it is expected that the rate of transformation is relative fast with respect to the incubation time for the transformation (development of a stable Mn_3O_4 nucleus). Hence, the number of MnO precipitates and Mn_3O_4 precipitates will be large compared to the number of partially transformed precipitates. This is indeed the case, but still some partially transformed precipitates were observed (*cf.* Figs 4 and 6).

4.2. Orientation relation between Cu and Mn_3O_4

The mismatch between Mn_3O_4 and Cu is anisotropic; the *a*-axis of the tetragonal spinel is 12.6% and the *c*-axis is 30.3% longer than twice the lattice constant of Cu. Analogous to Mn_3O_4 precipitates in Ag [2], the plate-shaped precipitates with (001) as dominant facet, as expected on the basis of strain energy, are not observed; the shape is dominated by {111} facets, e.g. is an octahedron (near parallelism of principal axis) or is a plate (near 71°{011}). The same reasoning for the occurrence of these shapes may hold as for Mn_3O_4 in Ag [2]. However, probably more important for the present case is that the shapes of the Mn_3O_4 precipitates are determined predominantly by the original shapes of the MnO precipitates out of which the Mn_3O_4 form. Influence on the Mn_3O_4 precipitates in Ag is only exerted by the matrix, whereas influence on Mn_3O_4 precipitates in Cu is exerted both by the matrix and by MnO. This results in a less straight-forward behavior, particular with respect to the 'rotation' (see Ref. [2]) of the precipitates in the matrix, for Mn_3O_4 precipitates in Cu than in Ag.

The influence of the transformation out of MnO on Mn_3O_4 nucleation and growth is expected to be substantial, because only diffusion of Mn is in principle necessary with a final effect that the (tetragonal distorted) face-centered close packed O lattice of Mn_3O_4 is only related by a Bain strain lattice correspondence to the f.c.c. O lattice of MnO with the *a*-axis −8.4% and the *c*-axis +6.0%. Also, half of all Mn atoms can remain on their sites and a quarter has to shift less than the nearest neighbor Mn–O distance in MnO and finally only a quarter has to diffuse out of the structure. Thus, although the MnO to Mn_3O_4 transformation needs long-range diffusion for a quarter of all Mn atoms, it is not surprising that it resembles a martensitic transformation for instance by the tetragonal twinning observed in the Mn_3O_4 precipitates (*cf.* Figs 5 and 6).

Using the phenomenological analysis of martensitic transformation by matrix algebra, e.g. the Bowles–Mackenzie theory [21, 22], with the values of the Bain strain relating Mn_3O_4 to MnO gives as result that an invariant plane is impossible in this case. Reason for the absence of an invariant plane is the significant reduction in volume associated with the Bain distortion, which is only possible because the 'unit cell' loses a quarter of all Mn atoms by long-range diffusion. Both diffusion and volume reduction are generally not compatible with martensitic transformations.

An invariant line [23, 24] is of course possible due to the mixed signs of the strains and corresponds to any direction on the cone making an angle of 41.2° with the '*c*-axis' in MnO (angle is readily obtained from the equality: $(0.916a)^2+(1.060c)^2=a^2+c^2$). After the Bain distortion these invariant-line directions constitute a cone making an angle of 37.1° with the *c*-axis of Mn_3O_4 and thus if MnO and Mn_3O_4 lattices are related by an invariant line they are related by a rotation of 4.1° around the [*hk*0] perpendicular to the invariant-line direction. In case of isotropic elasticity and no preferred slip direction or no slip related to accommodation of strains by plastic deformation, any plane containing an invariant line can be the habit plane relating the lattices before and after transformation [24]. In the realistic case of anisotropic elasticity the habit plane can be assumed to contain the most soft [*hk*0] direction and the invariant line that is perpendicular to this soft direction. In case accommodation of strains by plastic deformation occurs, the habit plane can be assumed to contain the [*hk*0] with highest Schmid factor on the active slip plane and the invariant line at the intersection of the slip plane and the cone of unextended lines. These predictions for the habit plane were derived for coherent plate-shaped pre-

cipitates and assumed to correspond to the condition of minimum strain energy [23, 24]. A discussion on this assumed minimum energy basis of the invariant-line model is given in Appendix A. For MnO the ⟨100⟩ are soft (based on the fact that $2c_{44}/(c_{11}-c_{12})>1$) and the habit plane expected in case of coherence is about {087}.

The angles between crystal zone axes of Cu and Mn_3O_4 as observed experimentally from SAED and Kikuchi patterns clearly indicate that the type of rotation expected for an invariant-line habit-plane is actually present, but instead of caused by the MnO to Mn_3O_4 transformation may be caused by a low-energy orientation of the Mn_3O_4 precipitate in the Cu matrix as was observed for these precipitates in the Ag matrix as described in a preceding paper [2]. Then the expected rotation is, as for Mn_3O_4 in Ag, 3.83° around ⟨110⟩ which is parallel in metal and oxide. However, from SAED (Kikuchi patterns) it follows that not the ⟨110⟩ (together with the ⟨112⟩) are parallel in Cu and Mn_3O_4 corresponding to a mismatch of 12.6%, but the ⟨011⟩ is in general parallel (then the ⟨211⟩ is not parallel) which corresponds to a mismatch of 21.8%. Also, observed parallelism of planes between Cu and Mn_3O_4 (*cf.* Section 3) strongly indicates that this is caused by the transformation from MnO to Mn_3O_4 and not by a low-energy orientation of Mn_3O_4 in Cu.

However, predictions from the invariant-line model [23, 24] do not seem to apply strictly. A reason can be that MnO and Mn_3O_4 are not *only* related by the Bain strain lattice correspondence, but also have different composition, crystallography and cations with different oxidation state and this is not accounted for by the continuum elasticity approach of the invariant-line. This limits the predictive capability of the invariant-line model. Most corresponding lattice planes in MnO and Mn_3O_4 have different composition, crystallography and/or polarity and if present as habit plane should in one way or another be associated with a certain defect structure. Since the oxygen sublattices in MnO and Mn_3O_4 are *only* related by the Bain distortion a habit plane completely consisting out of anions does not give rise to this defect structure. Such a habit plane is energetically more favorable, even if some deviation from the invariant-line condition occurs, than a habit plane exactly containing an invariant line but also introducing defects. Planes defined by three odd indices (smallest possible integers, zero is even) are such planes only containing oxygen ions. This hardly poses restrictions if high index planes are allowed (e.g. {100} can be approximated by {911}), but this also indicates that such planes are not much different from the habit planes associated with defects and are thus not favorable (the separation between the dissimilar lattice planes in MnO and Mn_3O_4 across the habit plane becomes small). Low-index planes with odd indices which also make an angle with the c-axis relatively close to the one defining the Bain cone are {111} and {133}. This may be an explanation for the observed parallelism of these planes in Cu and Mn_3O_4.

During the transformation of MnO to Mn_3O_4 the influence of the matrix is a second order effect and Cu/Mn_3O_4 interfaces are formed which are not in a low energy state. The image shown in Fig. 4 can be interpreted as to point in this direction. After transformation is completed at the relative high internal oxidation temperatures close to the melting point of the metal matrix, the Mn_3O_4 precipitates may be reoriented in the matrix to obtain a minimum energy state (if the activation-energy barrier for reorientation is overcome). Then the analogy between Cu/Mn_3O_4 and Ag/Mn_3O_4 should become more apparent. However, this is not observed. For a part caused by the change of a significant fraction ($30 \pm 10\%$) of MnO single-crystal precipitates into Mn_3O_4 precipitates containing several domains separated by tetragonal twin boundaries (see Figs 5 and 6) or by unidentified less regular grain boundaries (see Fig. 7) and for another part caused by the order of magnitude larger size of the precipitates in Cu compared to the ones in Ag, which diminish the influence of the strain and interfacial energy in case of Cu making loss of (semi-) coherency more likely than re-orientation to give low-energy semi-coherent interfaces.

5. CONCLUSIONS

Internal oxidation (2 to 24 h at 800 to 1000°C) of Cu–1 at.%Mn results in MnO precipitates mainly and a minor fraction (5–10%) Mn_3O_4 precipitates with a typical size of 200 nm. The OR's predominantly found are cube-on-cube and 71°⟨011⟩ corresponding, respectively, to precipitates with octahedron shape and plate shape with a {111} as dominant facet. The Mn_3O_4 develops in Cu by transformation out of MnO in contrast with the direct nucleation of Mn_3O_4 in Ag. Thermodynamically Mn_3O_4 is, also for small coherent or semi-coherent precipitates, more stable than MnO and the presence of MnO in Cu is a consequence of growth kinetics. The OR between Mn_3O_4 and Cu is mainly determined by the OR between MnO and Mn_3O_4 developing during transformation, which is largely influenced by the presence of a cone of unextended lines (Bain cone) for these two oxide phases with largely equivalent crystal lattices. Starting from an OR between MnO and Cu, the OR between the transformed Mn_3O_4 and Cu can develop into different variants related by rotations of the order of a few degrees. If a single-crystalline MnO precipitate transforms in Mn_3O_4 with more than one nucleation site these different OR variants generally lead to a polycrystalline Mn_3O_4 precipitate containing low-angle grain boundaries.

Acknowledgements—The work described in this paper is part of the research program of the Foundation for Fundamental Research of Matter (FOM-Utrecht).

REFERENCES

1. Ernst, F., *Mater. Sci. Engng Rep. R*, 1995, **14**, 97.
2. Kooi, B. J., Groen, H. B. and De Hosson, J. Th. M., *Acta mater.*, 1997, **45**, 3587.
3. Ernst, F., *Mater. Res. Soc. Symp. Proc.*, 1990, **183**, 49.
4. Kooi, B. J., Groen, H. B., De Hosson, J. Th. M., *Acta mater.*, 1997, **46**, 111.
5. Rhines, F. N., *Trans. metall. Soc. A.I.M.E.*, 1940, **137**, 246.
6. Rhines, F. N., Johnson, W. A. and Anderson, W. A., *Trans. metall. Soc. A.I.M.E.*, 1942, **147**, 205.
7. Wyckoff, R. W. G., *Crystal Structures*, 2nd edn. Interscience Publishers, New York, 1963.
8. Kooi, B. J., De Hosson, J. Th. M., in *Proc. 5th Europ. Conf. Advanced Materials and Processes and Applications*, Vol. 4, ed. L. A. J. L. Sarton, H. B. Zeedijk, Euromat, 1997, p. 17.
9. Lu, P. and Cosandey, F., *Ultramicroscopy*, 1992, **40**, 271.
10. Jang, H., Seidman, D. N. and Merkle, K. L., *Interface Sci.*, 1993, **1**, 61.
11. Chen, F. R., Chiou, S. K., Chang, L. and Hong, C. S., *Ultramicroscopy*, 1994, **54**, 179.
12. Vellinga, W. P. and De Hosson, J. Th. M., *Mater. Sci. Forum 209*, 1996, **207**, 361.
13. Chan, D. K., Seidman, D. N. and Merkle, K. L., *Phys. Rev. Let.*, 1995, **75**, 1118.
14. Vellinga, W. P., Ph.D. thesis, University of Groningen, 1996.
15. Megusar, J. and Meier, G. H., *Metall. Trans. A*, 1976, **7A**, 1133.
16. Kapteijn, J., *Z. Metallk.*, 1974, **65**, 157.
17. Meijering, J. L., in *Adv. mater. Res.*, ed. H. Herman, 1971, Vol. 5, p. 1.
18. Verfurth, J. E. and Rapp, R. A., *Trans. metall. Soc. A.I.M.E.*, 1964, **230**, 1310.
19. Barin, I., Knacke, O., *Thermochemical Properties of Inorganic Substances*. Springer-Verlag, Berlin, 1973.
20. Hirth, J. P., Lothe, J., *Theory of dislocations*. McGraw-Hill, New York, 1968.
21. Bowles, J. S., Mackenzie, J. K., *Acta metall.*, 1954, Vol. 2, pp. 124, 129, 138.
22. Nishiyama, Z., *Martensitic Transformation*. Academic Press, 1978.
23. Dahmen, U., *Acta metall.*, 1982, **30**, 63.
24. Dahmen, U. and Westmacott, K. H., *Acta metall.*, 1986, **34**, 475.
25. Duly, D., *Acta metall. mater.*, 1993, **41**, 1559.
26. Kato, M. and Fuji, T., *Acta metall. mater.*, 1994, **42**, 2929.
27. Willis, J. R., Jain, S. C. and Bullough, R., *Phil. Mag. A*, 1990, **62**, 115.
28. Bollmann, W., *Crystal Defects and Crystalline Interfaces*. Springer, New York, 1970.
29. Burgers, W. G., *Physica*, 1934, **1**, 561.

APPENDIX A

Minimum Energy Basis Of The Invariant-line Model

As was already recognized in Ref. [24] and shown in Refs [25, 26], the true condition of minimum strain energy would need a stress-free line instead of a strain-free line. Considering this problem and based on the observation that the habit plane for a number of experimental cases does not correspond to minimum strain energy and is better predicted by using the invariant-line approach, in Ref. [25] the conclusion is drawn that energetic considerations do not allow to justify the invariant-line model (and alternative explanations for the presence of invariant lines in habit planes were searched for). This conclusion is indeed justified in case of fully coherent interfaces. However, the invariant-line approach is often applied (with fair success) to cases of Bain strains of (±)5% and larger and this also holds for the experimental cases considered in Ref. [25]. Then a fully coherent interface is, apart from really thin plates (below the critical thickness [27], see below), hardly possible and a semi-coherent interface involving misfit dislocations, usually of edge-type (because edge dislocations relieve mismatch along parallel directions most efficiently) must be considered. Dahmen *et al.* also consider 'semi-coherent' inclusions [24], but then semi-coherence implies the occurrence of plastic deformation along a (irrational) slip direction on a specific slip plane and this is a case different from the one presently considered.

One edge dislocation and also a parallel array of edge dislocations yields a state of plane strain with as normal the line direction of the dislocation(s) [20]. Hence, the mismatch at a habit plane or interface containing an invariant line can be relieved by a one-dimensional array of parallel edge dislocations perpendicular to the invariant line (*i.e.* in [*hk*0] direction). This is impossible if the habit plane was constituted by a stress-free line instead of a strain-free line. Then, a 2-dimensional network of edge dislocations, *e.g.* based on the O-lattice [28], must be present. Now the invariant-line approach can be based on minimum energy if it can be shown that the energy pertaining to the one-dimensional array of misfit dislocations in case of a (nearly) strain-free line is lower than the energy pertaining to the 2-dimensional network of dislocations in case this line is not present. According to a model developed [27] this can indeed be shown in case of a nearly invariant line, but does not hold in case of the exact invariant line.

For instance, for an epitaxial layer with thickness h on a semi-infinite substrate the elastic energy per unit length of dislocation (x_3-axis) in a cell confined by $\pm p/2$ along the direction of the dislocation array with p as repeat distance (x_1-axis) and from $-\infty$ to h (from substrate side to free surface of layer) along a direction perpendicular to the interface (x_2-axis) can be described by [27] (also adopting their use of symbols):

$$pE = E_d + E_c - \tfrac{1}{2} ph\overline{\sigma_{ij}}\varepsilon_{ij}^{r1} \qquad \text{(A.1)}$$

with E_c the energy of the dislocation cores which are assumed isolated, E_d the energy of the (overlapping) dislocations derived from the resolved stress in the plane $\vec{x}_2 - \vec{r}$ ($\int \sigma_{fl}{}^{d} b_f \, dx_2$), ε_{ij}^{r1} the tensor containing the relaxed strains (original strains based on the mismatch at the interface ε_{ij}^{r1} are relaxed due to introduction of the array of dislocations) and $\overline{\sigma_{ij}}$ is mean stress generated by ε_{ij}^{r1}. Minimum energy results in an equilibrium state where a certain amount of strain is relaxed by the introduction of an array of dislocations with a certain p and a certain amount of strain remains. For a certain system (with certain materials constants) this depends critically on the original mismatch strains and the layer thickness; the transition from a fully coherent to a semi-coherent epitaxial layer is marked by a critical thickness.

For a 2-dimensional network, *e.g.* two arrays both exactly similar to the one in equation (A.1) and at right angles to one another, equation (A.1) is modified to [27]:

$$pE = 2E_d + 2E_c - \tfrac{1}{2} ph\overline{\sigma_{ij}}\varepsilon_{ij}^{r2} \qquad \text{(A.2)}$$

where E_d and E_c are unchanged with respect to equation (A.1) and thus simply additive for 2 non-parallel arrays. Only the relaxed strains and the subsequently generated mean stresses are affected by changing from one to two arrays, because relaxed by contributions from each

array. For two arrays of edge dislocations at right angles to one another, the only mutual interaction from both directions is due to Poisson contraction exerted by the mean (relaxed) stresses.

The mismatch or strain along one direction of any interface between two phases related by tetragonal transformation strains, *i.e.* along the [*hk*0], is fixed. Only by rotation around [*hk*0] the amount of strain along the direction perpendicular to [*hk*0] can be varied (in between the positive and negative value of the Bain strains). Using equations (A.1) and (A.2) (where equation (A.2) is restricted by only considering edge dislocations and generalized by allowing all possible networks of edge dislocations) it can now be derived that the minimum energy orientation of an interface between two phases related by tetragonal transformation strains too large to be accommodated fully coherently is such that a one-dimensional array of edge dislocations is present along [*hk*0] that relax the strain in this direction to such an extent that the residual principal stress which remains necessary in this direction by means of Poisson contraction exactly relieves the strain that is present in a direction perpendicular to the [*hk*0] direction. This perpendicular direction will then be in-between the orientations corresponding to the stress-free line and the strain-free line, but nearer to the strain-free line, since it can be expected that the array of edge dislocations relaxes most of the strain along the [*hk*0]. In this way all the long-range stress/strains are relieved at the interface and the present minimum energy state does not only apply to an infinite thin plate as is usually the case for the coherent inclusion problem. Only in case all mismatch along [*hk*0] is relaxed by the misfit dislocation array (this non-equilibrium state will not occur because the more the mismatch is relaxed the less driving force remains to introduce new dislocations and make the repeat distance between them smaller) then the minimum energy state will occur for an interface containing the invariant line exactly. It is expected that the general [*hk*0] will be restricted to the specific crystallographic direction of the most likely Burgers vector in the soft system, *e.g.* the $\frac{1}{2}$[110] in f.c.c. systems.

An example given in Ref. [25] to illustrate that minimum strain energy is not observed experimentally can now be seen in a different perspective. For the b.c.c./h.c.p. couple Mo/Mo_2C the rotation needed to form a habit plane containing a stress-free line is 11.73°, to contain a strain-free line is 4.90° and the experimentally observed rotation is 5.26°, which is in-between the rotations for a stress and strain-free line, but much nearer to the strain-free line, which agrees with the present expectation. Particularly, because the Bain strains for the Mo to Mo_2C transformation correspond to −4.6% for the *a*-axis and +6.1% for the *c*-axis and are thus relatively large to give full coherent instead of semi-coherent interfaces (which of course can be verified using HRTEM). However, the accuracy of the experimentally observed rotation is probably ± 0.5° and the specific value of 5.26° is given, because this rotation brings two low-index directions in the b.c.c. and h.c.p. phases parallel independently from the relative lattice parameters of both phases and corresponds to the well-known Burgers OR [29].

This also illustrates a limitation of predicting habit planes on the basis of a stress or strain-free line or the one in-between proposed here, because they are based on linear continuum elasticity and do not account properly (particularly in case of the stress-free line) for influence of crystallography, interfacial energy differences for different habit planes when excluding the effect of stress/strains, *etc.* This limited usefulness of the continuum approach is particularly invoked, if the approach is applied, as is often done, to predicting habit planes between two phases which are not related by a Bain-strain lattice correspondence only, but to phases which also have different compositions. In completely metallic couples the influence of composition differences is probably not prominent, but in couples where ionic or covalent bonds are present, charged defects arising at certain predicted habit planes or just the interfacial energy (excluding strain energy) of the habit plane may be far more important than strain energy for such a habit plane. This was already shown for the Mn_3O_4 precipitates in Ag [2] and in Cu (Section 4.2). Only in case influence of stress/strain for relatively small strains still has predominant influence on the total energy of an interface region, first to be expected for completely metallic couples, elastic strain energy minimization can be expected successful for the prediction of habit planes.